Supporting information

# Ensembles from Silver Clusters and Cucurbit[6]urils-contained Linkers

Na-Na Li,[a,b] Ming Yang,[b] Xiao-Jie Xu,[c] Xi-Yan Dong,[*a,b] Si Li[*b] and Shuang-Quan Zang[a,b]

[a]College of Chemistry and Chemical Engineering, Henan Polytechnic University Henan Key Laboratory of Coal Green Conversion, Henan Polytechnic University, Jiaozuo 454000, China

[b]Henan Key Laboratory of Crystalline Molecular Functional Materials, Henan International Joint Laboratory of Tumor Theranostical Cluster Materials, Green Catalysis Center, and College of Chemistry, Zhengzhou University, Zhengzhou 450001, China

[c]School of Physics and Electronic Information Engineering, Henan Polytechnic University, Jiaozuo 454000, China

E-mail: dongxiyan0720@hpu.edu.cn, lisi@zzu.edu.cn

**Table S1.** Crystal data and structure refinements for **NC a** and **SCM 1**.

| | **NC a** | **SCM 1** |
|---|---|---|
| CCDC number | 2095834 | 2095835 |
| Empirical | $C_{78}H_{98}Ag_{12}N_6O_{22}S_{12}$ | $C_{100}H_{119.96}Ag_{12}N_{28}O_{36}S_{14}$ |
| Formula weight | 3150.78 | 4033.48 |
| Temperature/K | 200.00(10) | 200.00(10) |
| Crystal system | monoclinic | monoclinic |
| Space group | $P2_1/n$ | $P2/c$ |
| $a$ /Å | 15.88620(10) | 14.7785(17) |
| $b$ /Å | 12.60960(10) | 15.0645(13) |
| $c$ /Å | 25.3661(2) | 29.008(3) |
| $\alpha$ /° | 90 | 90 |
| $\beta$ /° | 94.1890(10) | 92.988(10) |
| $\gamma$ /° | 90 | 90 |
| Volume /Å$^3$ | 5067.73(7) | 6449.3(11) |
| $Z$ | 2 | 2 |
| $\rho_{calc}$ g/cm$^3$ | 2.065 | 2.077 |
| $\mu$/mm$^{-1}$ | 21.029 | 17.144 |
| F(000) | 3080.0 | 3984.0 |
| Radiation | Cu K$\alpha$ ($\lambda$ = 1.54184) | Cu K$\alpha$ ($\lambda$ = 1.54184) |
| Reflections collected | 26038 | 34606 |
| Independent reflections | 9910 [$R_{int}$ = 0.0356, $R_{sigma}$ = 0.0399] | 12669 [$R_{int}$ = 0.0865, $R_{sigma}$ = 0.0725] |
| Data/restraints/parameters | 9910/109/678 | 12669/1083/1331 |
| Goodness-of-fit on F$^2$ | 1.048 | 1.072 |
| Final R indexes [I>=2$\sigma$ (I)] | $R_1$ = 0.0323, $wR_2$ = 0.0827 | $R_1$ = 0.1317, $wR_2$ = 0.3430 |
| Final R indexes [all data] | $R_1$ = 0.0360, $wR_2$ = 0.0850 | $R_1$ = 0.1558, $wR_2$ = 0.3621 |

$\boldsymbol{R_1 = \sum||F_o|-|F_c||/\sum|F_o|}$, $\boldsymbol{wR_2 = [\sum w(F_o^2 - F_c^2)^2/\sum w(F_o^2)^2]^{1/2}}$

**Table S2.** Crystal data and structure refinements for **SCM 2** and **SCM 3**.

| | **SCM 2** | **SCM 3** |
|---|---|---|
| CCDC number | 2095836 | 2095837 |
| Empirical | $C_{137}H_{150.5}Ag_{12}F_{24}N_{32.5}O_{33.5}S_6$ | $C_{88}H_{148}Ag_{12}N_{32}O_{40}S_{14}$ |
| Formula weight | 4731.19 | 4037.66 |
| Temperature/K | 200.00(10) | 199.99(10) |
| Crystal system | monoclinic | triclinic |
| Space group | $P2_1/n$ | $P$-1 |
| $a$ /Å | 15.29384(8) | 13.9198(2) |
| $b$ /Å | 25.34019(12) | 14.8144(2) |
| $c$ /Å | 21.44672(10) | 18.0353(2) |
| $\alpha$ /° | 90 | 79.5070(10) |
| $\beta$ /° | 90.4025(5) | 80.7700(10) |
| $\gamma$ /° | 90 | 79.2250(10) |
| Volume /Å$^3$ | 8311.44(7) | 3561.59(8) |
| $Z$ | 2 | 1 |
| $\rho_{calc}$ g/cm$^3$ | 1.890 | 1.883 |
| $\mu$ /mm$^{-1}$ | 12.715 | 15.546 |
| F(000) | 4688.0 | 2008.0 |
| Radiation | Cu K$\alpha$ ($\lambda$ = 1.54184) | Cu K$\alpha$ ($\lambda$ = 1.54184) |
| Reflections collected | 89844 | 37672 |
| Independent reflections | 16623 [$R_{int}$ = 0.0451, $R_{sigma}$ = 0.0302] | 13836 [$R_{int}$ = 0.0719, $R_{sigma}$ = 0.0673] |
| Data/restraints/parameters | 16623/660/1405 | 13836/64/956 |
| Goodness-of-fit on F$^2$ | 1.024 | 1.033 |
| Final R indexes [I>=2$\sigma$ (I)] | $R_1$ = 0.0392, $wR_2$ = 0.1003 | $R_1$ = 0.0631, $wR_2$ = 0.1750 |
| Final R indexes [all data] | $R_1$ = 0.0452, $wR_2$ = 0.1003 | $R_1$ = 0.0736, $wR_2$ = 0.1808 |

$$R_1 = \sum||F_o|-|F_c||/\sum|F_o|,\ wR_2 = [\sum w(F_o^2 - F_c^2)^2/\sum w(F_o^2)^2]^{1/2}$$

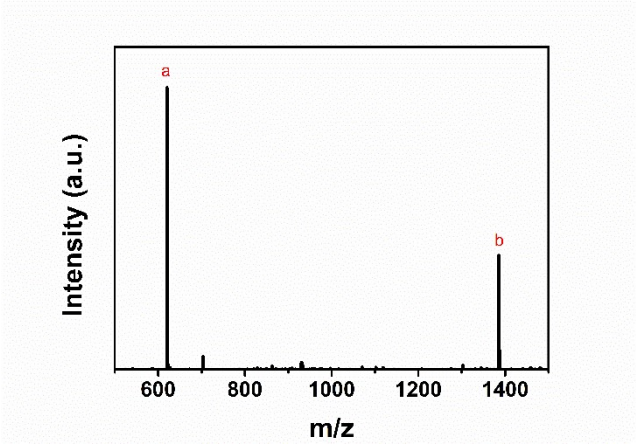


**Fig. S1.** ESI-MS spectrum of the solution of **L·PF$_6$** (obtained from dissolving **L·PF$_6$** in DMF) in the positive mode.

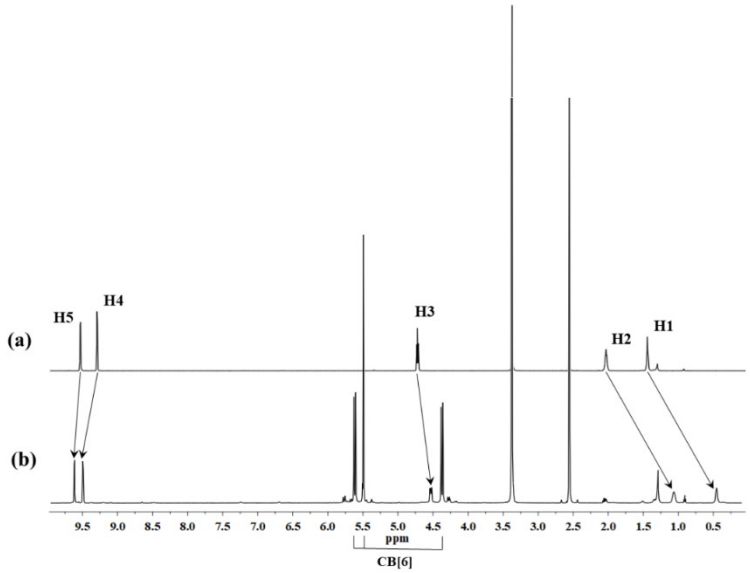


**Fig. S2.** $^{1}$H NMR spectra of (a) the guest molecule BPHB and (b) the pseudorotaxane **L·PF$_6$** in $(CD_3)_2SO$.

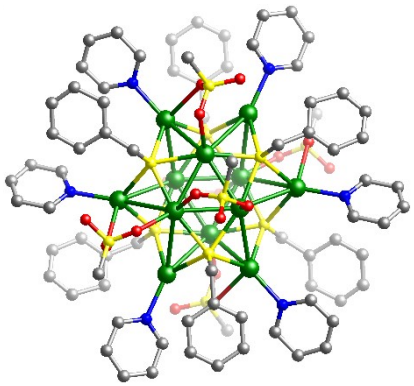

**Fig. S3.** The crystal structure of **NC a**. Color labels: Ag, green; S yellow; N, blue; C, gray; O, red.

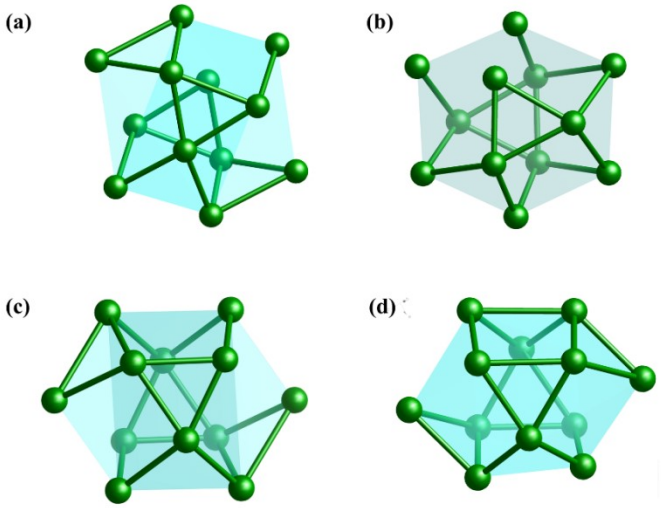


**Fig. S4.** Perspective view of the $D_{3d}$ cuboctahedron in the $Ag_{12}S_6$ core skeleton with Ag3–Ag6–Ag3 three-layer arrangement in (a) **NC a** and (b-c) **SCM 1-3**. Color labels: Ag, green.

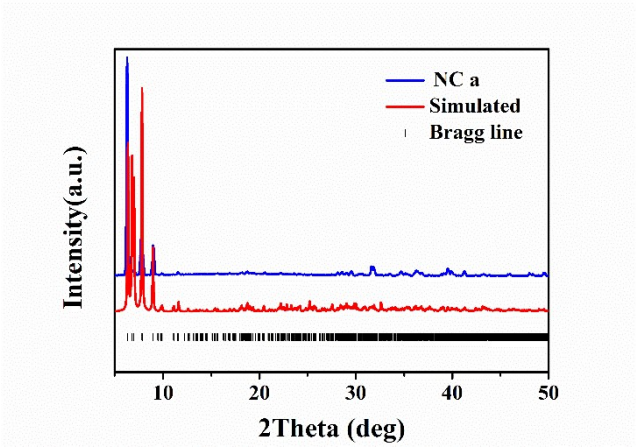


**Fig. S5.** PXRD patterns of **NC a**.

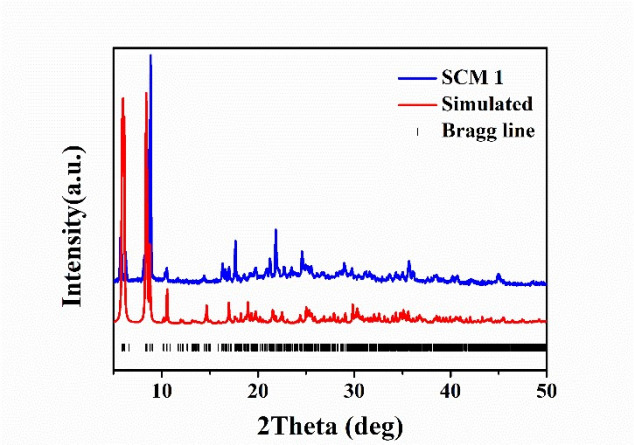


**Fig. S6.** PXRD patterns of **SCM 1**.

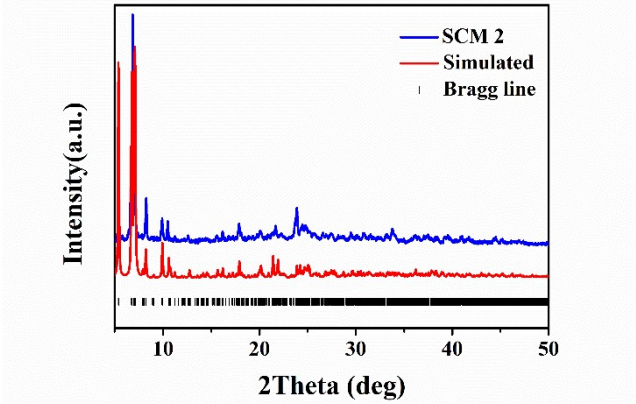


**Fig. S7.** PXRD patterns of **SCM 2**.

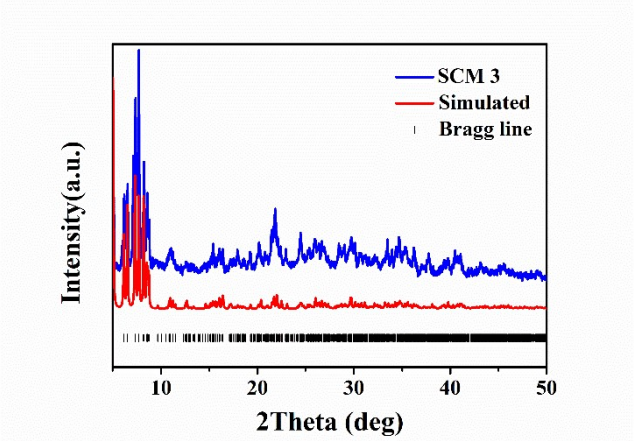


**Fig. S8.** PXRD patterns of **SCM 3**.

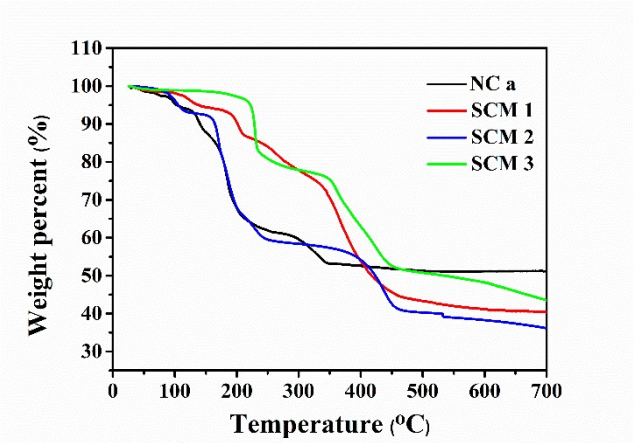


**Fig. S9.** The TGA curves for **NC a** and **SCM 1-3**.

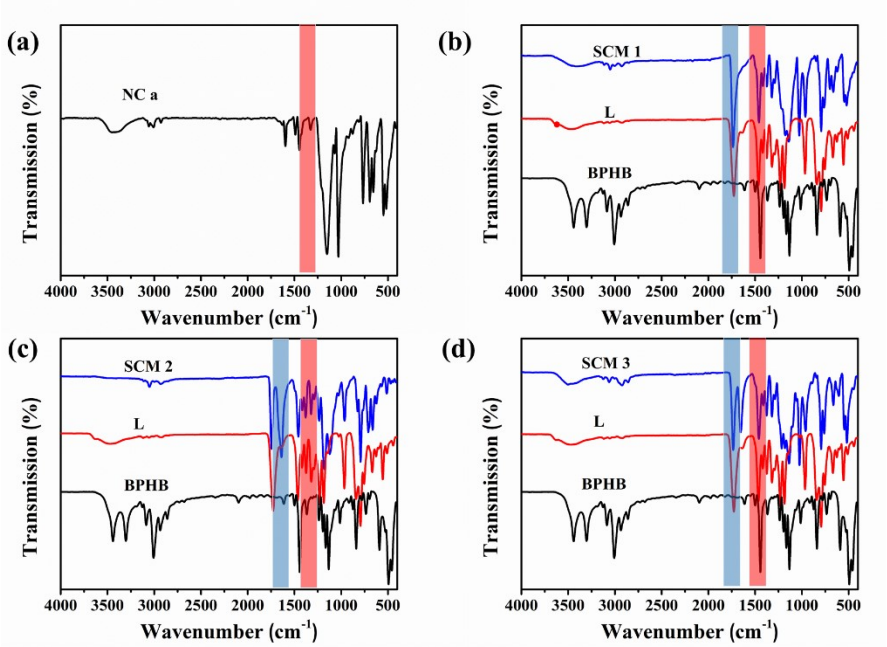


**Fig. S10.** (a) The IR spectrum of **NC a**. (b) The IR spectra of **SCM 1**, **L·PF$_6$**, and BPHB. (c) The IR spectra of **SCM 2**, **L·PF$_6$** and BPHB. (d) The IR spectra of **SCM 3**, **L·PF$_6$** and BPHB.

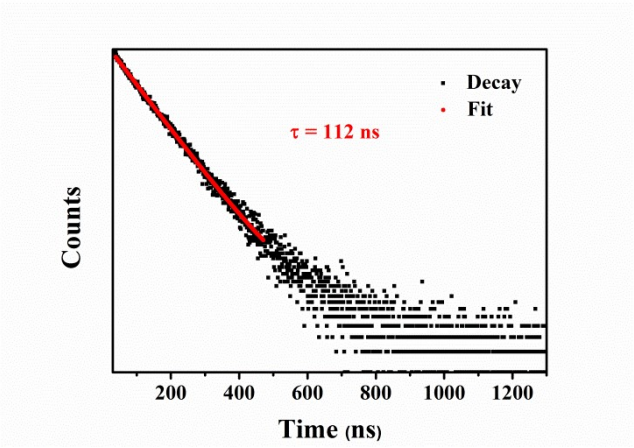


**Fig. S11.** Emission lifetime of **NC a** measured at 575 nm at 298 K.

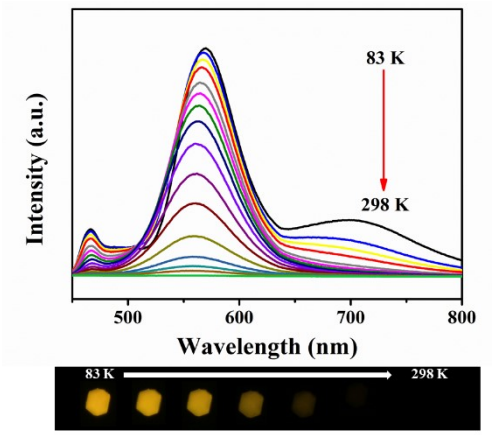


**Fig. S12.** Variable-temperature emission spectra and crystal luminescence photographs of **NC a**.

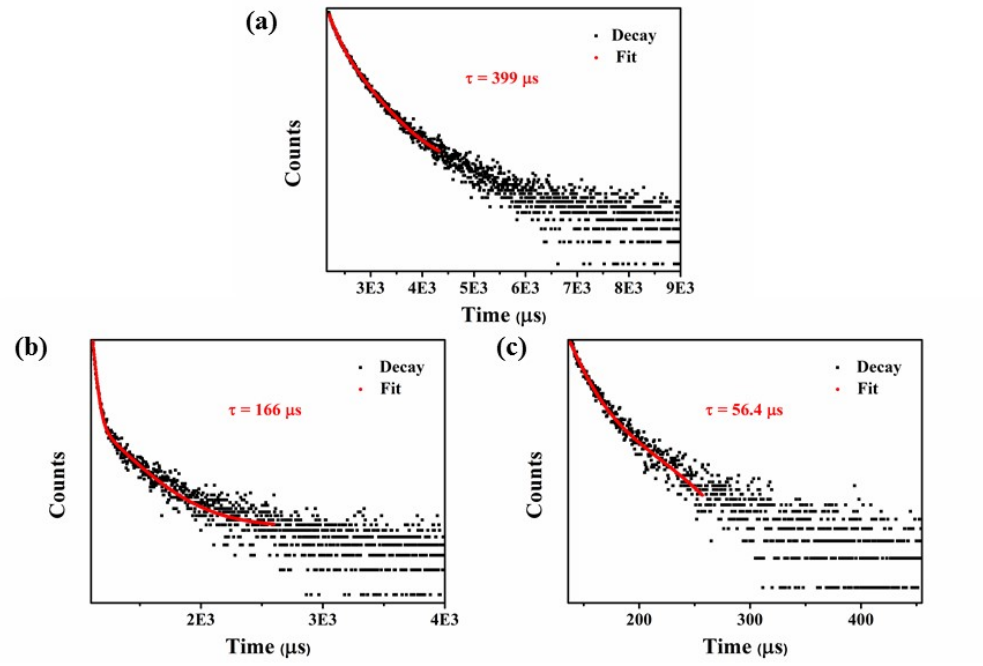


**Fig. S13.** Photoluminescence decay profile of **NC a** measured at (a) 465nm, (b) 570 nm, and (c) 704 nm at 83 K.

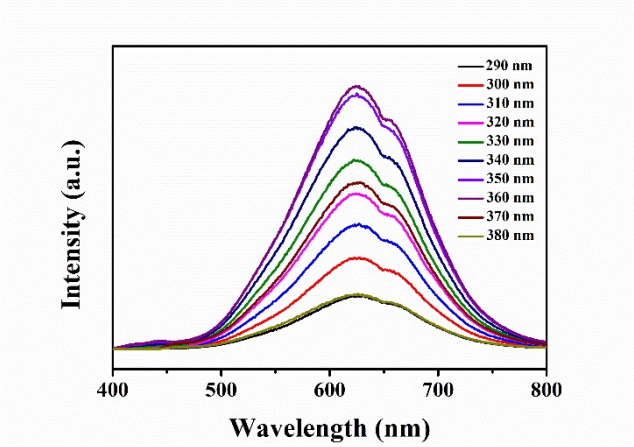


**Fig. S14.** Solid-state emission spectra of **SCM 1** at different excitation wavelengths at room temperature.

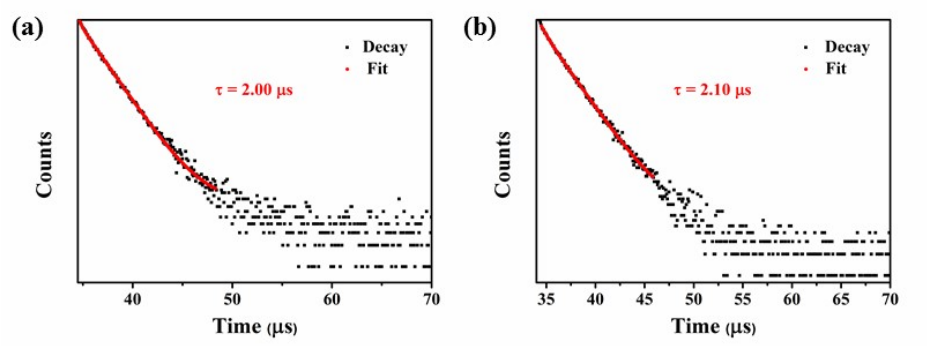


**Fig. S15.** Emission lifetime of **SCM 1** measured at (a) 630 nm and (b) 656 nm at 298 K.

**Table S3.** The rate of radiative transition ($k_r$) and non-radiative transition ($k_{nr}$) of T1 state were obtained according to following equations (assuming the efficiency of intersystem crossing is 100%), where $\Phi$ represents the corresponding quantum yield:

$$k_{nr} + k_r = 1/\tau$$

$$k_r = \Phi(k_{nr} + k_r)$$

| compound | $\Phi$ | $\tau$ | $k_r$ ($s^{-1}$) | $k_{nr}$ ($s^{-1}$) |
|---|---|---|---|---|
| **NC a** | 0.22 % | 120 ns | $1.83x10^4$ | $8.33x10^6$ |
| **SCM 1** | 4.88 % | 2.00 μs($\lambda_{em}$ = 630 nm) | $2.44x10^4$ | $4.76x10^5$ |
| **SCM 2** | 0.18 % | 92.9 ns | $1.94x10^4$ | $1.08x10^7$ |
| **SCM 3** | 4.04 % | 67.6 ns($\lambda_{em}$ = 572 nm) | $5.98x10^5$ | $1.48x10^8$ |

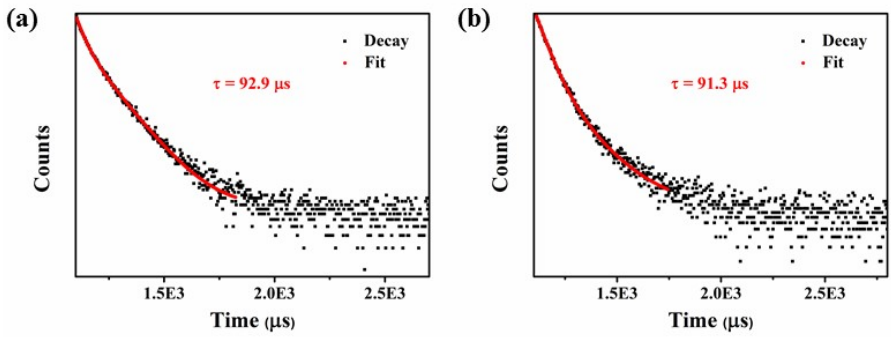


**Fig. S16**. Photoluminescence decay profile of **SCM 1** measured at (a) 585 nm and (b) 672 nm at 83 K.


**Fig. S17.** Fluorescence photos of **SCM 1-3** under the exposure time of 3.25 s.

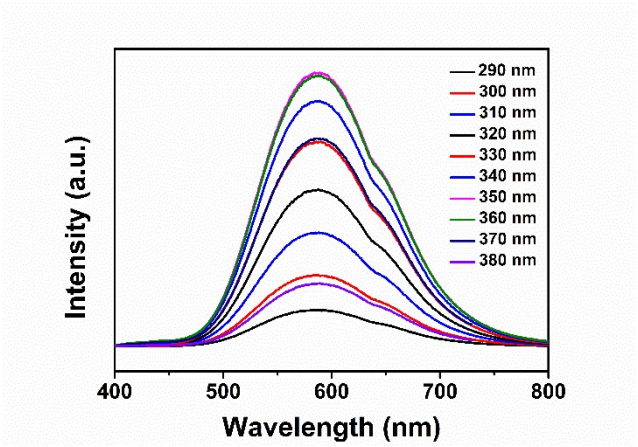


**Fig. S18.** Solid-state emission spectra of **SCM 3** at different excitation wavelengths at room temperature.

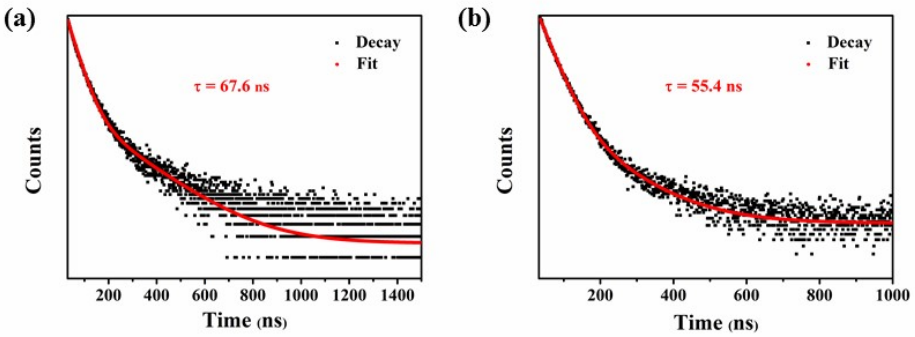


**Fig. S19.** Emission lifetime of **SCM 3** at measured at (a) 572 nm and (b) 655 nm at 298 K.

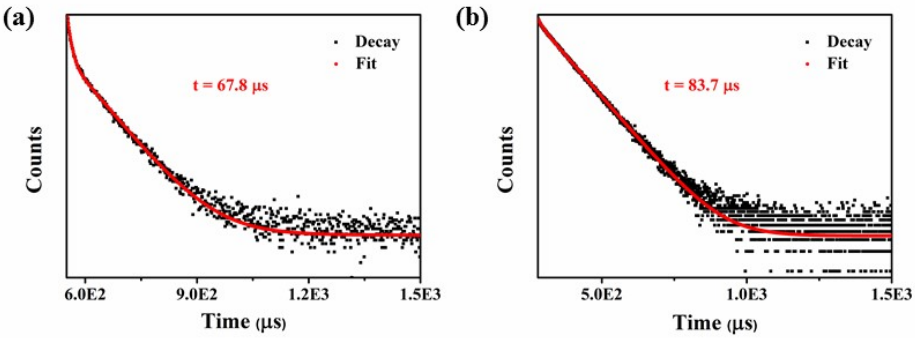


**Fig. S20.** Photoluminescence decay profile of **SCM 3** measured at (a) 583 nm and (b) 655 nm at 83 K.

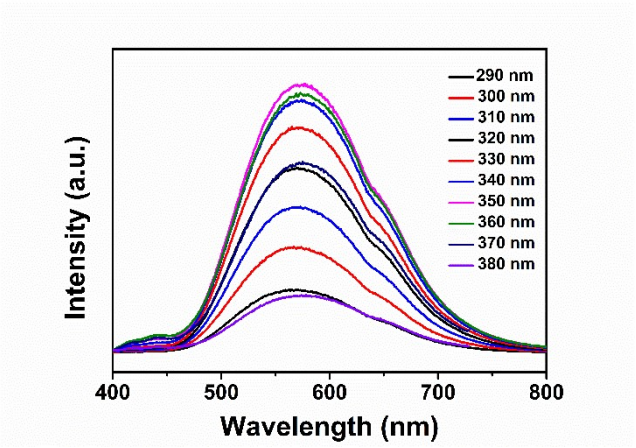


**Fig. S21.** Solid-state emission spectra of **SCM 2** at different excitation wavelengths at room temperature.

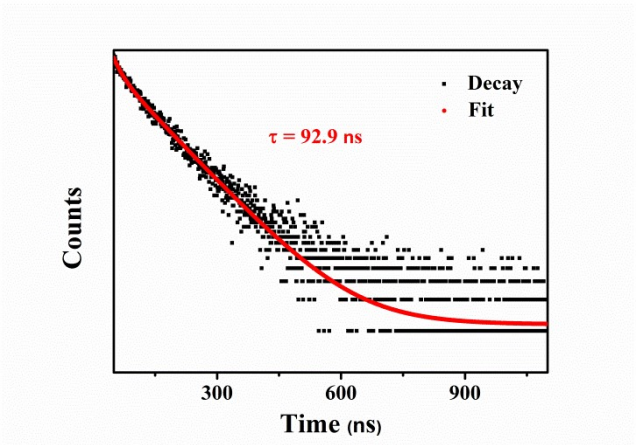


**Fig.22.** Emission lifetime of **SCM 2** measured at 578 nm at 298 K.

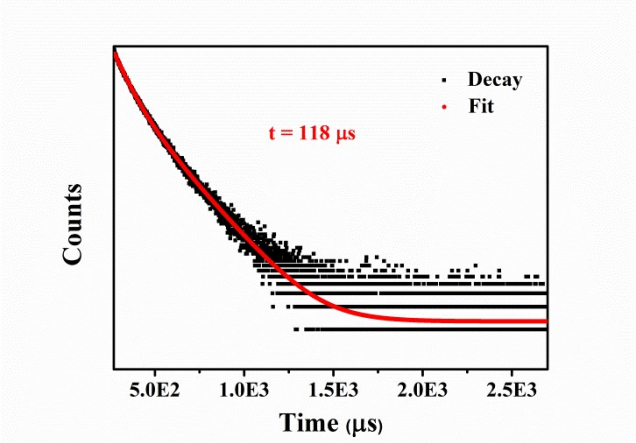


**Fig. S23.** Photoluminescence decay profile of **SCM 2** measured at 610 nm at 83 K.

**Table S4.** Emission wavelength ($\lambda_{em}$), lifetimes ($\tau$) and the corresponding fractional contributions (%) of the solid-state samples at 298 k and 83 k, respectively ($\chi$2: fitting parameter).

| **Compound-298K** | $\lambda_{em}$ | $\chi^2$ | $\tau_1$(%) | $\tau_2$(%) | $\tau$ |
|---|---|---|---|---|---|
| **NC a** | 575 nm | 1.00 | 112 ns(100) | | 112 ns |
| **SCM 1** | 630 nm | 1.04 | 0.305 μs(7.01) | 2.14 μs(92.99) | 2.00 μs |
| | 656 nm | 0.98 | 0.668 μs(4.63) | 2.20 μs(95.37) | 2.10 μs |
| **SCM 2** | 578 nm | 0.94 | 20.3 ns(13.18) | 104 ns(86.82) | 92.9 ns |
| **SCM 3** | 572 nm | 1.16 | 176 ns(22.04) | 37.1 ns(77.96) | 67.6 ns |
| | 655 nm | 1.16 | 36.3 ns(78.69) | 126 ns(21.31) | 55.4 ns |
| **Compound-83 K** | $\lambda_{em}$ | $\chi^2$ | $\tau_1$(%) | $\tau_2$(%) | $\tau$ |
| **NC a** | 465 nm | 1.11 | 156 μs(26.74) | 487 μs(73.26) | 399 μs |
| | 580 nm | 1.19 | 26.4 μs(44.77) | 279 μs(55.23) | 166 μs |
| | 704 nm | 1.06 | 79.9 μs(64.26) | 14.1 μs(35.74) | 56.4 μs |
| **SCM 1** | 585 nm | 1.15 | 36.5 μs(28.12) | 115μs(71.88) | 92.9 μs |
| | 672 nm | 1.04 | 55.5 μs(64.22) | 156 μs(35.78) | 91.3 μs |
| **SCM 2** | 610 nm | 1.00 | 69.4 μs(48.14) | 163 μs(51.86) | 118 μs |
| **SCM 3** | 583 nm | 1.19 | 9.42 μs(20.01) | 82.4 μs(79.99) | 67.8 μs |
| | 655 nm | 1.18 | 17.0 μs(2.92) | 85.7 μs(97.08) | 83.7 μs |